

NACA RM L55107



~~CONFIDENTIAL~~

Copy 5
RM L55107

~~FOR REFERENCE~~
NACA

NOT TO BE TAKEN FROM THIS ROOM

RESEARCH MEMORANDUM

TRANSONIC WIND-TUNNEL INVESTIGATION OF THE
EFFECTS OF EXTERNAL STORES AND STORE POSITION ON THE
AERODYNAMIC CHARACTERISTICS OF A 1/16-SCALE MODEL OF
THE DOUGLAS D-558-II RESEARCH AIRPLANE

By Thomas C. Kelly

Langley Aeronautical Laboratory
Langley Field, Va.

CLASSIFICATION ~~CHANGED~~

UNCLASSIFIED

To: _____

By authority of *NACA Kelly* *effective*
RN-178 Date *Jan 24, 1958*

AT 8-13-58

CLASSIFIED DOCUMENT

LANGLEY AERONAUTICAL LABORATORY

This material contains information affecting the National Defense of the United States within the meaning of the espionage laws, TITLE 18, U.S.C., Secs. 793 and 794, the transmission or revelation of which in any manner to an unauthorized person is prohibited by law.

NATIONAL ADVISORY COMMITTEE FOR AERONAUTICS

WASHINGTON

November 8, 1955

CONFIDENTIAL

[REDACTED]

NATIONAL ADVISORY COMMITTEE FOR AERONAUTICS

RESEARCH MEMORANDUM

TRANSONIC WIND-TUNNEL INVESTIGATION OF THE
EFFECTS OF EXTERNAL STORES AND STORE POSITION ON THE
AERODYNAMIC CHARACTERISTICS OF A 1/16-SCALE MODEL OF
THE DOUGLAS D-558-II RESEARCH AIRPLANE

By Thomas C. Kelly

SUMMARY

An investigation has been conducted in the Langley 8-foot transonic tunnel to determine the effects of adding external, pylon-suspended stores to a 1/16-scale model of the Douglas D-558-II research airplane. Tests were made for two spanwise store locations and covered a Mach number range from 0.60 to 1.15 and angles of attack from approximately -2° to 12° .

Results indicated that the drag increment at transonic speeds which resulted from adding stores in an outboard (0.61-semispan) location could be reduced somewhat by positioning the stores at an inboard (0.44-semispan) location thereby obtaining an improvement in the longitudinal area development for a Mach number of 1.0. Lift-curve slopes, which were increased at subsonic speeds by the addition of stores, were reduced at Mach numbers above about 0.91 and 1.07 for the configurations tested with stores in the outboard and inboard positions, respectively.

A destabilizing pitching-moment break for the basic configuration was eliminated at Mach numbers from 0.60 to 0.85 over the range of lift coefficients tested by addition of stores at the outboard position. The undesirable pitching-moment condition was present, however, and in some cases aggravated for the configuration with stores at the inboard location. A general decrease in stability accompanied the addition of stores in either position.

INTRODUCTION

A general research program established to study the effects of adding pylon-suspended stores to the Douglas D-558-II research airplane is

[REDACTED]

currently in progress. As part of this program, a store-pylon combination has been tested on a 1/16-scale model of the D-558-II in the Langley 8-foot transonic tunnel. Two wing-semispan store locations were investigated in order to study the effects of adding external stores and to determine if a lower transonic drag level could be obtained with the stores in a position which resulted in the more desirable $M = 1.0$ longitudinal area development. (See ref. 1.)

Results of these tests are presented herein at Mach numbers from 0.60 to 1.15 and angles of attack from approximately -2° to 12° . Reynolds numbers for the present tests were on the order of 1.8 million.

Results of tests at subsonic and supersonic speeds for some identical models may be found in references 2 and 3.

SYMBOLS

C_D	drag coefficient, D/qS
C_{D_0}	drag coefficient at zero lift
ΔC_D	incremental drag coefficient, $C_{D_{\text{model with stores}}} - C_{D_{\text{model without stores}}}$
ΔC_{DF}	incremental drag coefficient based on store frontal area, $\Delta C_D \frac{S}{2F}$
C_L	lift coefficient, L/qS
$C_{L(L/D)_{\text{max}}}$	lift coefficient for maximum lift-drag ratio
$\frac{\partial C_L}{\partial \alpha}$	lift-curve slope per degree, averaged from $C_L = 0$ over linear portion of curve
C_m	pitching-moment coefficient, $\frac{M_{\bar{c}}/4}{qS\bar{c}}$
$\frac{\partial C_m}{\partial C_L}$	static-longitudinal-stability parameter, averaged from $C_L = 0$ over linear portion of curve

\bar{c}	wing mean aerodynamic chord, in.
D	drag, lb
F	store frontal area, sq ft
L	lift, lb
$(L/D)_{\max}$	maximum lift-drag ratio
M	free-stream Mach number
$M_{\bar{c}}/4$	pitching moment about $0.25\bar{c}$, in-lb
P_b	base pressure coefficient, $\frac{P_b - p}{q}$
P_b	static pressure at model base, lb/sq ft
p	free-stream static pressure, lb/sq ft
q	free-stream dynamic pressure, lb/sq ft
S	wing area, including that part within the fuselage, sq ft
α	angle of attack of fuselage center line, deg

APPARATUS

Tunnel

The Langley 8-foot transonic tunnel is a single return, dodecagonal slotted-throat wind tunnel designed to obtain aerodynamic data through the speed of sound while minimizing the usual effects of blockage. The tunnel, more completely described in reference 4, operates at a stagnation pressure which is close to atmospheric.

Model Support System

The model was mounted on an internal electrical strain-gage balance and was sting supported in the tunnel. A sting angular coupling was used to offset the model slightly from the tunnel center line at 0° angle of attack and to keep it near the center line at higher angles of attack.

Model

The 1/16-scale model of the D-558-II airplane with external stores mounted at the inboard position is shown in figure 1. Model details and design dimensions are presented in figure 2 and table I and area distributions for the model with and without stores are shown in figure 3. The model fuselage was circular in cross section and employed a vee-type canopy mounted well forward. The wing, which was mounted slightly above the horizontal fuselage center line, was at an angle of incidence of 3° and had 3° of negative dihedral. The wing had the 30-percent-chord line of the unswept panel swept back 35° , an aspect ratio of 3.57, a taper ratio of 0.565, and NACA 63-010 airfoil sections perpendicular to the chord line. The horizontal tail, which had airfoil sections identical to those of the wing, was mounted at 0° incidence with respect to the fuselage center line and had 40° sweepback of the 30-percent-chord line of the unswept panel. The vertical tail employed identical airfoil sections and had the chord line swept back 49° .

Stores and pylons were constructed using ordinates supplied by the Douglas Aircraft Company, Inc. Details are provided in figure 4. The fin-stabilized store, which is a 1/16-scale model of a 1,000-pound low-drag general-purpose bomb, had a fineness ratio of 8.56 and corresponds to store A of reference 2 and the small DAC store of reference 3. Stores were mounted on 66° sweptforward pylons having streamwise thickness ratios of 7.6 percent.

The model used for the present tests differed from the full-scale airplane in several respects: the fuselage base diameter was increased by 25 percent to allow sufficient clearance about the sting support; the model wing had constant NACA 63-010 airfoil sections normal to the 30-percent-chord line of unswept panel while the full-scale airplane employs sections varying from the NACA 63-010 at the root to NACA 63-012 at the tip; and the model was tested without the nose-pressure-tube-boom arrangement used on the full-scale airplane.

MEASUREMENTS AND ACCURACY

Lift, drag, and pitching moment were determined by means of the internal electrical strain-gage balance. Coefficients are based on the total wing area of 0.684 square foot. Pitching-moment coefficients, based on a mean aerodynamic chord of 5.46 inches, are referred to the quarter point of the mean aerodynamic chord. Based upon a consideration of the design load limits for the strain-gage balance and scatter of the data, measured coefficients are estimated to be accurate within the following limits:

C_L	± 0.01
C_D	± 0.001 to ± 0.002
C_m	± 0.004

As noted in reference 3, the possible error in drag coefficient is somewhat high because of low balance sensitivity with respect to axial-force measurements; however, the consistency of the data indicates that the probable maximum error in drag coefficient was of the order of ± 0.001 . Measurements of static pressure at the model base were made using an orifice located on the sting support just forward of the plane of the model base. Base pressure coefficients (fig. 5) determined from these measurements, are estimated to be accurate within ± 0.005 .

Model angle of attack was measured by means of a fixed-pendulum strain-gage unit located in the sting support and a calibration of sting and balance deflection under various loadings and is estimated to be accurate within $\pm 0.1^\circ$.

TESTS AND CORRECTIONS

Each configuration was tested at Mach numbers from 0.60 to 1.15. The angle-of-attack range was generally from approximately -2° to 12° , with the maximum attainable angle at a Mach number of 1.15 restricted because of sting-strength limitations. Reynolds numbers for the test were on the order of 1.8×10^6 (fig. 6). The basic model was tested without stores, with the stores at the 61-percent-semispan station (outboard), and with the stores at the 44-percent-semispan station (inboard).

A consideration of the results presented in reference 5 indicated that the effects of sting interference for a comparable model of the D-558-II were confined to drag and pitching moment. For the present investigation the effects on drag have been reduced by adjusting the data to a condition representing free-stream static pressure at the model base. No attempt was made to evaluate sting interference effects on pitching moments and the data are presented in an unadjusted form. The addition of stores would not be expected to change sting interference effects on pitching moments, however, and so comparisons of pitch characteristics between the configurations tested are valid.

Subsonic boundary-interference effects in the slotted test section are considered negligible and no corrections for these effects have been applied. In an effort to reduce the effects of supersonic boundary-reflected expansion and compression waves, the model was tested in a position vertically offset from the tunnel center line at an angle of

attack of 0° , (this procedure reduces shock-focusing effects), and in addition, the analysis figures plotted against Mach number have been faired to approximate a condition free of boundary-reflected disturbances.

RESULTS AND DISCUSSION

Basic force and moment data are presented in figures 7 to 9. Analysis figures, obtained from the basic plots, are presented as figures 10 to 14. In order to facilitate presentation of the data, staggered scales have been used in some figures, and care should be taken in selecting the zero axis for each curve.

Drag Characteristics

Comparison of the drag results of the present tests with those made at the Langley 7- by 10-foot tunnel (ref. 2) indicates fair agreement. Differences in the low-lift drag level between identical models tested at the two facilities may be attributed to differences in model surface condition. Results of the present investigation are in very good agreement with results obtained by adjusting the drag data of reference 5 to the condition of free-stream static pressure at the model base. It should be noted that the model of the present tests differed slightly from that of reference 5 in that the present model employed a raised canopy and enlarged vertical tail.

Comparison of drag results of the present tests with those of tests made at other NACA facilities, including full-scale flight results, may be found in reference 6. Extension of these comparisons (made at Mach numbers to about 1.6) to a Mach number of 2.0 may be made using the results of references 3 and 7.

Variations with Mach number of zero-lift drag coefficients for the model with stores off, and with the stores in the outboard and inboard positions are shown in figure 10. At subsonic speeds, adding stores in either semispan location increased the drag level by approximately 17 percent. The peak drag coefficient (near a Mach number of 1.12) for the basic configuration was increased by about 20 and 17 percent for the model tested with stores outboard and inboard, respectively. The slight improvement in the peak drag for the configuration with stores inboard would be expected from a consideration of the longitudinal cross-sectional-area developments shown in figure 3 for the configurations tested. The maximum cross-sectional-area peak for the configuration with stores inboard is seen to be lower than that for the model tested with stores outboard. Using the readily available $M = 1.0$ area developments, the method presented in reference 8 has been applied in an effort to estimate values of drag coefficients for the three configurations at a Mach

number of 1.0. The estimated coefficients for the model without stores, with stores outboard, and with stores inboard are 0.0758, 0.0975, and 0.0819, respectively. Quantitative agreement between the theoretical and experimental results is poor, as would be expected from results shown in reference 8. However, qualitative agreement is provided.

Incremental drag coefficients, based on both wing area and store frontal area are presented in figure 11 for a lift coefficient of zero. Data in the upper part of the figure for the stores tested in the outboard position are in fair agreement with data for the same model tested at $\alpha = -2^\circ$ ($C_L \approx 0$) in the Langley 7- x 10-foot tunnel. Incremental drag coefficients shown in the lower part of figure 11 for one store and pylon provide a comparison between results of the present test and unpublished results for the isolated store obtained from helium gun tests. The difference between the curve for the isolated store and the results of the present test represents the drag of the isolated pylon plus interference drag associated with the various components. If the drag coefficient for the isolated pylon (based on store frontal area) is assumed to be 0.14 at supersonic speeds, the interference drag coefficient for the complete configuration (2 stores and pylons) at $M = 1.15$, for example, would be 1.36 for the configuration with inboard stores as compared with 1.72 for the configuration with outboard stores. Based on wing area, these coefficients would be 0.0083 and 0.0105 for the inboard and outboard locations, respectively. Similarly, the interference drag is seen to be substantially lower for the stores inboard configuration at all other Mach numbers investigated.

The variations of drag coefficient with Mach number at lift coefficients of 0.3 and 0.6, shown in figure 12 for the three configurations, are similar to those noted at zero lift. At these lift coefficients, however, the drag rise begins earlier and is more severe than that indicated at zero lift.

Maximum lift-drag ratios and lift coefficients for maximum lift-drag ratio are presented in figure 13. Lift-drag ratios for the model tested without stores varied from approximately 11 at subsonic speeds to 4 at a Mach number of 1.12. Adding stores resulted in a reduction in maximum lift-drag ratios throughout the Mach number range, the greatest losses occurring for the configuration tested with stores in the outboard position. The losses in lift-drag ratio resulting from adding stores were accompanied by a general increase in the lift coefficient required for maximum lift-drag ratio.

Lift and Pitching-Moment Characteristics

Adding stores in either semispan position resulted in a positive shift in the angle of zero lift. (See figs. 7(a), 8(a), and 9(a)).

Lift-curve slopes (fig. 14) which were increased at subsonic speeds by the addition of stores, were reduced at Mach numbers above about 0.91 and 1.07 for the configurations tested with stores in the outboard and inboard positions, respectively.

Examination of the pitching-moment curves presented in figures 7(c) and 8(c) indicates that, over the range of lift coefficients tested, adding stores in the outboard (0.61-semispan) position eliminated the destabilizing break seen in the pitching-moment curves of the basic configuration at Mach numbers from 0.60 to 0.85. The data of reference 2 indicate, however, that the pitching-moment break may still exist but is delayed to lift coefficients higher than those obtained in the present tests. Comparison of the results presented in figure 9(c) with those shown in figures 7(c) and 8(c) indicates that with the stores at the inboard (0.44-semispan) station the undesirable break was present and, in some cases, more abrupt than that for the model without stores. Results similar to those noted above may be found in reference 9, wherein pylon suspended nacelles were tested at two wing-semispan locations (0.60b/2 and 0.50b/2). The pylons used in reference 9 had leading edges swept forward 66.2° and were mounted at a chordwise location comparable to that of the present tests.

Comparison of the pitch results for the present tests with those of reference 2 indicates an apparent change in trim for identical configurations. This change may be attributed to differences in the ratio of sting area to model base area for the two investigations. (See ref. 5.)

The variation of the static-longitudinal-stability parameter with Mach number, shown in figure 14, indicates that adding stores to the basic configuration resulted in a general decrease in stability at low lift coefficients throughout the Mach number range, with the exception of a slight increase noted for the configuration with stores inboard at Mach numbers from 0.98 to 1.15.

CONCLUSIONS

The following may be concluded from results of tests at Mach numbers from 0.60 to 1.15 of a 1/16-scale model of the Douglas D-558-II research airplane:

1. The drag of the basic configuration was increased on the order of 20 percent at a Mach number of 1.12 as a result of adding pylon-suspended stores in an outboard (0.61-semispan) location. With the stores at an inboard (0.44-semispan) location, a slight reduction of the increment in drag due to adding stores was obtained as a result of an improvement in the longitudinal area development for a Mach number of 1.0.

2. Lift-curve slopes, taken over the low-lift range, were increased at subsonic speeds by the addition of stores and reduced at Mach numbers above about 0.91 and 1.07 for the configurations tested with stores in the outboard and inboard positions, respectively.

3. A destabilizing pitching-moment break for the basic configuration was eliminated at Mach numbers from 0.60 to 0.85 over the range of lift coefficients tested by addition of stores at an outboard (0.61-semispan) location. The undesirable condition was present, however, and in some cases aggravated for the configuration tested with stores at the inboard (0.44-semispan) location.

4. A general decrease in stability at low lift coefficients accompanied the addition of stores.

Langley Aeronautical Laboratory,
National Advisory Committee for Aeronautics,
Langley Field, Va., August 23, 1955.

REFERENCES

1. Whitcomb, Richard T.: A Study of the Zero-Lift Drag-Rise Characteristics of Wing-Body Combinations Near the Speed of Sound. NACA RM L52H08, 1952.
2. Silvers, H. Norman, and King, Thomas J., Jr.: Investigation at High Subsonic Speeds of the Effects of Various Underwing External-Store Arrangements on the Aerodynamic Characteristics of a 1/16-Scale Model of the Douglas D-558-II Research Airplane. NACA RM L55D11, 1955.
3. Smith, Norman F.: Exploratory Investigation of External Stores on the Aerodynamic Characteristics of a 1/16-Scale Model of the Douglas D-558-II Research Airplane at a Mach Number of 2.01. NACA RM L54F02, 1954.
4. Ritchie, Virgil S., and Pearson, Albin O.: Calibration of the Slotted Test Section of the Langley 8-Foot Transonic Tunnel and Preliminary Experimental Investigation of Boundary-Reflected Disturbances. NACA RM L51K14, 1952.
5. Osborne, Robert S.: High-Speed Wind-Tunnel Investigation of the Longitudinal Stability and Control Characteristics of a 1/16-Scale Model of the D-558-II Research Airplane at High Subsonic Mach Numbers and at a Mach Number of 1.2. NACA RM L9C04, 1949.
6. Purser, Paul E.: Comparison of Wind-Tunnel, Rocket, and Flight Drag Measurements for Eight Airplane Configurations at Mach Numbers Between 0.7 and 1.6. NACA RM L54F18, 1954.
7. Nugent, Jack: Lift and Drag Characteristics of the Douglas D-558-II Research Airplane Obtained in Exploratory Flights to a Mach Number of 2.0. NACA RM L54F03, 1954.
8. Holdaway, George H.: Comparison of Theoretical and Experimental Zero-Lift Drag-Rise Characteristics of Wing-Body-Tail Combinations Near the Speed of Sound. NACA RM A53H17, 1953.
9. Carmel, Melvin M., and Fischetti, Thomas L.: A Transonic Wind-Tunnel Investigation of the Effects of Nacelles on the Aerodynamic Characteristics of a Complete Model Configuration. NACA RM L53F22a, 1953.

TABLE I

DESIGN DIMENSIONS OF THE 1/16-SCALE MODEL OF THE D-558-II

Wing:	
Area, sq ft	0.684
Span, in.	18.72
Aspect ratio	3.57
Taper ratio	0.565
Mean aerodynamic chord, in.	5.46
Root chord, in.	6.78
Tip chord, in.	3.83
Sweep, deg (30-percent-chord line of unswept panel)	35
Incidence, deg	3
Dihedral, deg	-3
Airfoil section (normal to 30-percent-chord line of unswept panel)	NACA 63-010
Horizontal Tail:	
Area, sq ft	0.156
Span, in.	8.98
Aspect ratio	3.59
Taper ratio	0.50
Mean aerodynamic chord, in.	2.61
Sweep, deg (30-percent-chord line of unswept panel)	40
Dihedral, deg	0
Airfoil section (normal to 30-percent-chord line of unswept panel).	NACA 63-010
Vertical Tail:	
Area, sq ft	0.143
Span, in.	6.14
Sweep, deg (30-percent-chord line of unswept panel)	49
Airfoil section (normal to 30-percent-chord line of unswept panel)	NACA 63-010
Fuselage:	
Length, in.	31.5
Maximum diameter, in.	3.75
Fineness ratio	8.40
Base diameter, in.	1.56
Base area, sq ft	0.013
Ratio of fuselage base area to wing area	0.019
Store:	
Length, in.	7.50
Maximum diameter, in.	0.876
Fineness ratio	8.56
Frontal area, sq ft	0.0042
Ratio of store frontal area to wing area	0.0061



L-83364



L-83366

Figure 1.- The 1/16-scale Douglas D-558-II model with stores at the inboard position mounted in the Langley 8-foot transonic tunnel.

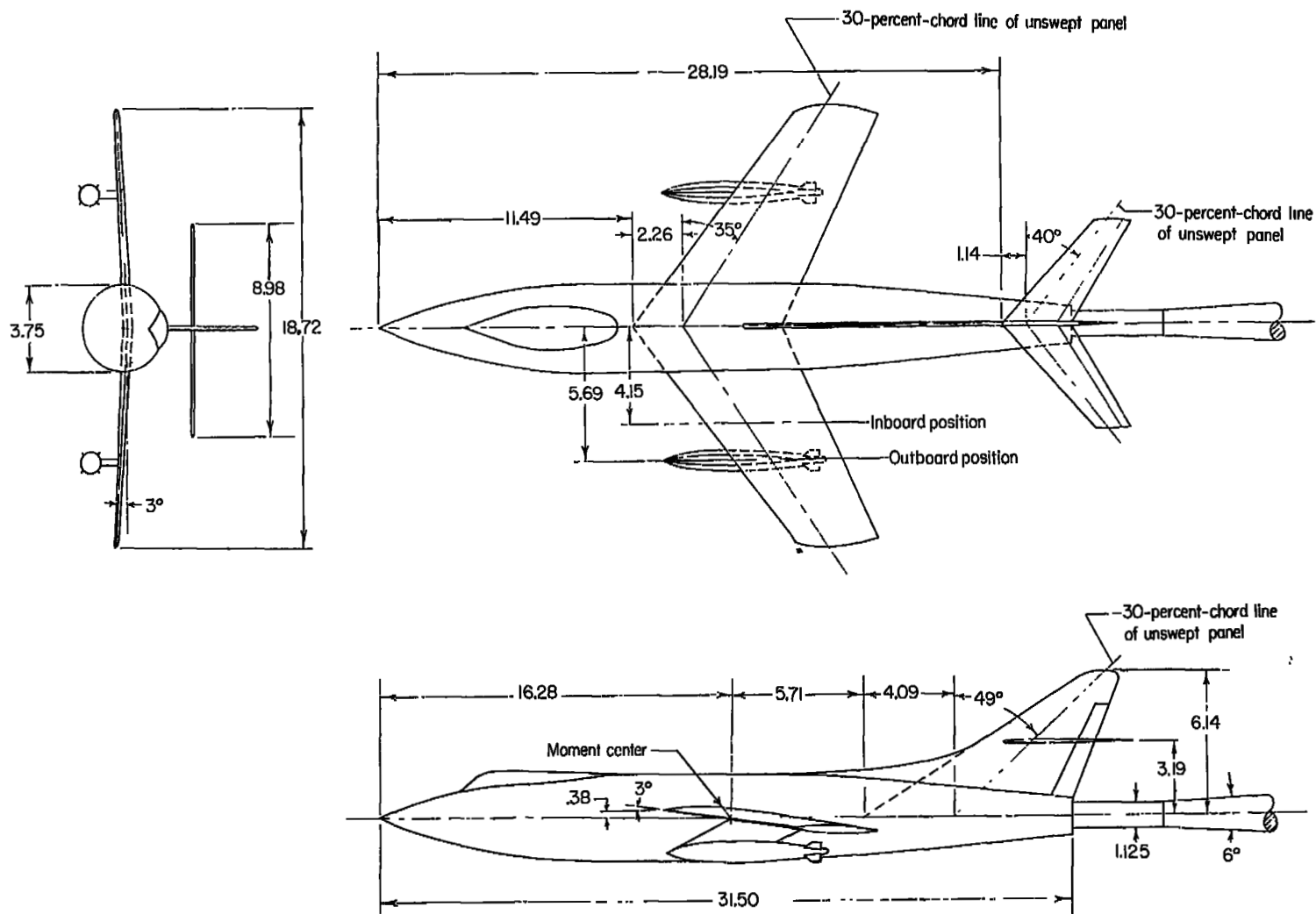


Figure 2.- Model details. All dimensions are in inches unless otherwise noted.

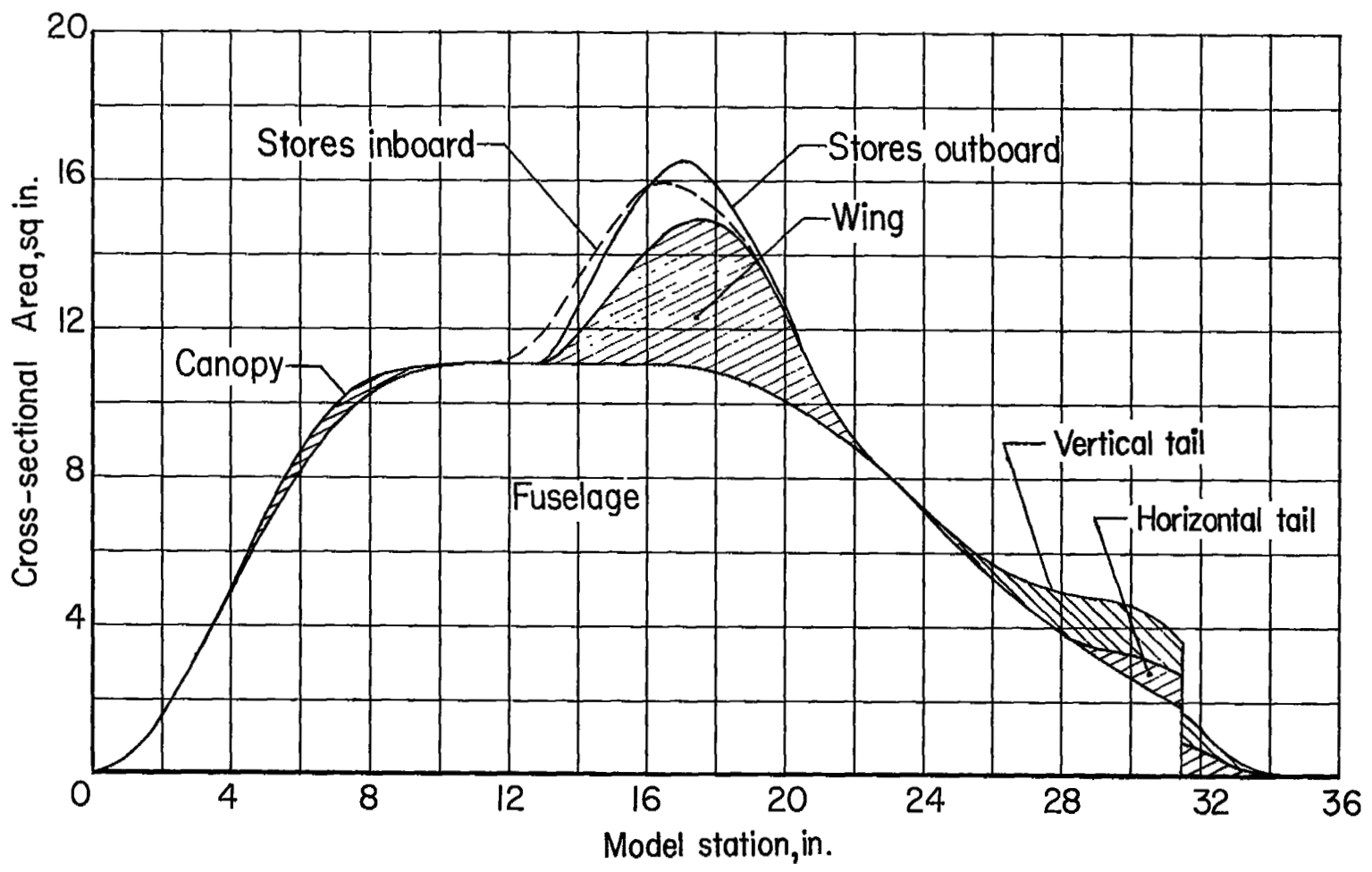
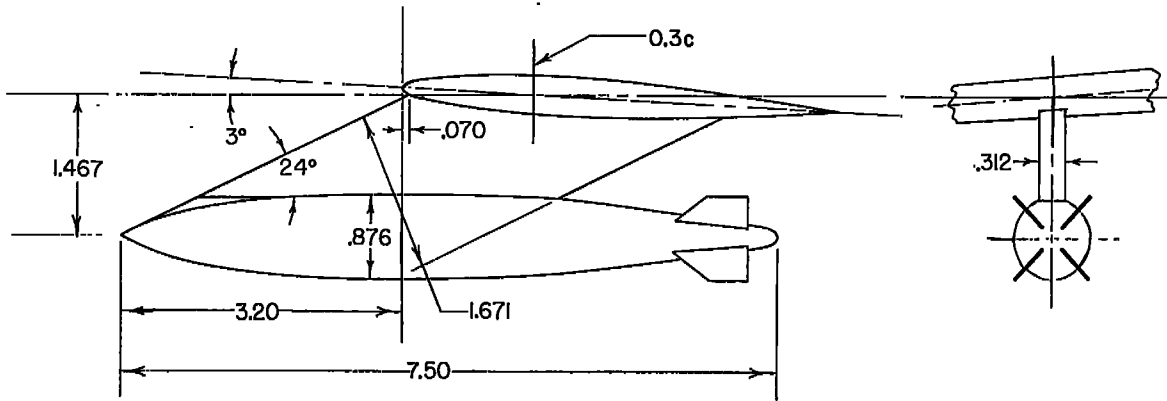


Figure 3.- Longitudinal cross-sectional area developments for the configurations tested.



Pylon Ordinates		Store Ordinates	
Station	Ordinate	Station	Radius
0	0	0	0
L.E. rad.	.017	L.E. rad.	.042
.031	.032	.146	.070
.063	.045	.354	.153
.156	.070	.563	.216
.313	.096	.772	.264
.468	.111	1.109	.332
.625	.128	1.605	.378
.782	.138	2.02	.412
.938	.146	2.23	.425
1.195	.152	2.44	.435
1.250	.155	2.65	.438
1.407	.156		
Straight line		Straight line	
2.11	.156	3.73	.438
2.56	.155	3.94	.436
2.72	.151	4.15	.432
2.88	.144	4.57	.413
3.03	.134	4.98	.385
3.19	.121	5.90	.347
3.34	.105	6.24	.302
3.66	.066	6.65	.257
3.97	.021	7.03	.197
4.12	0	7.20	.122
		7.36	.096
		T.E. rad.	.042
		7.50	0

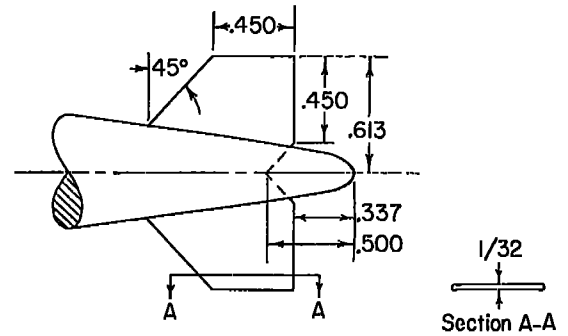


Figure 4.- Store and pylon details. All dimensions are in inches unless otherwise noted.

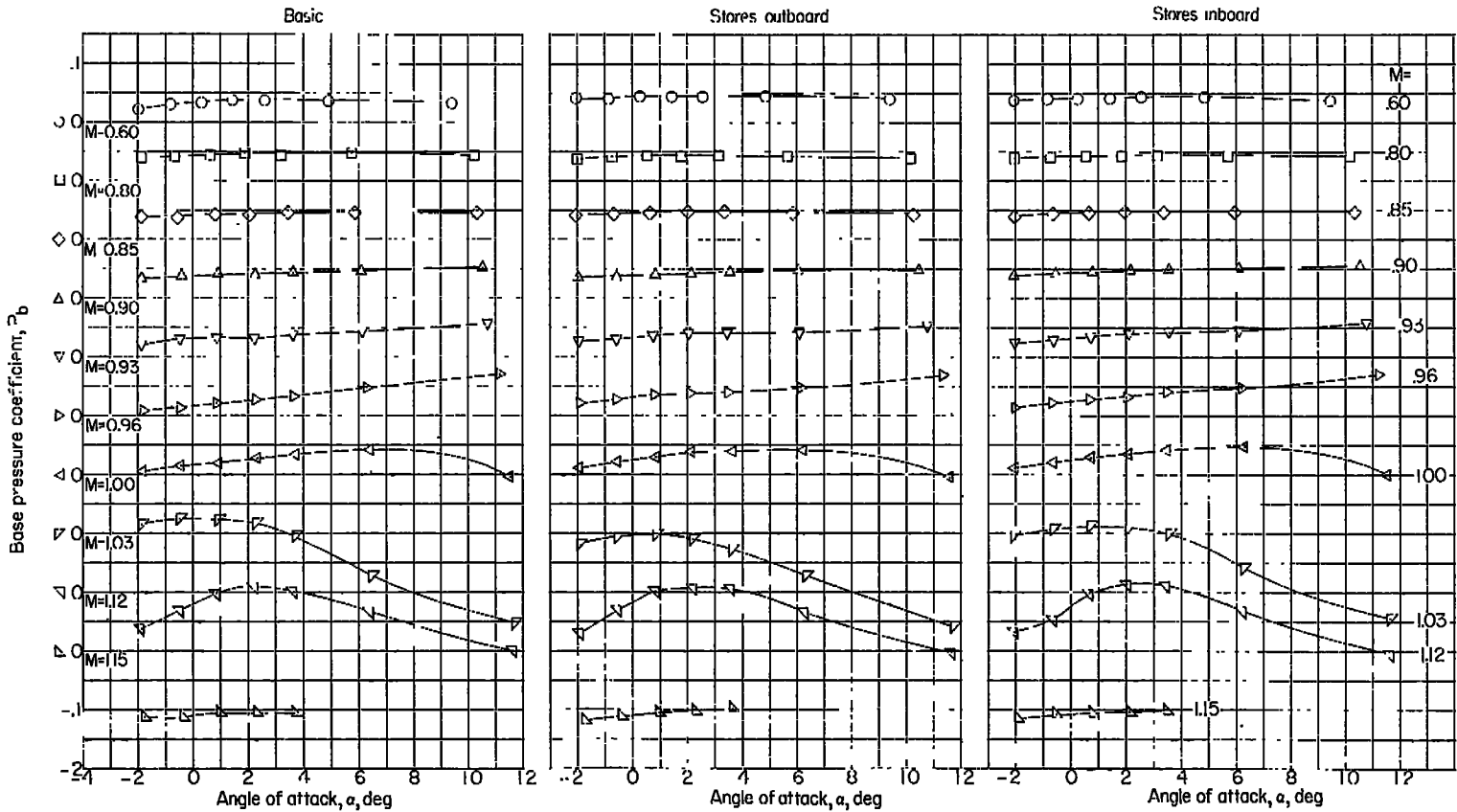


Figure 5.- Variation with angle of attack of model base pressure coefficients for several Mach numbers.

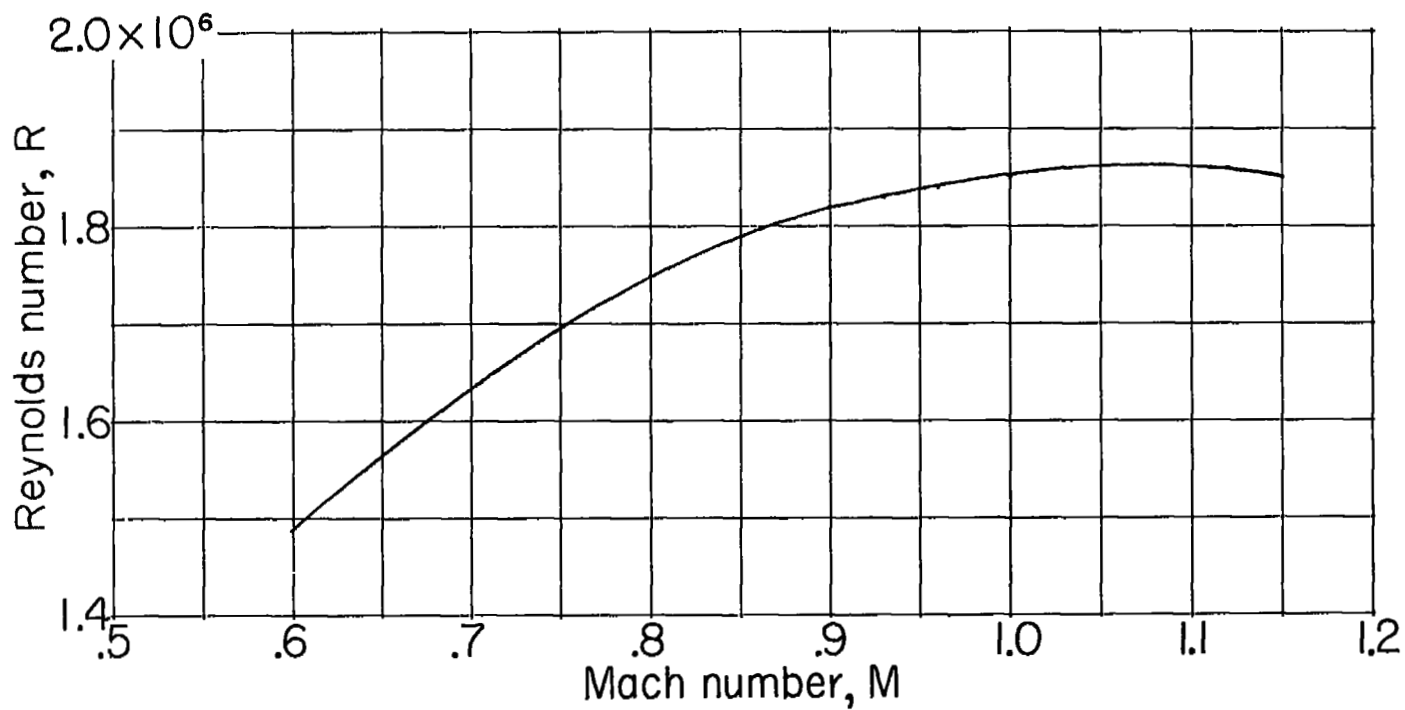
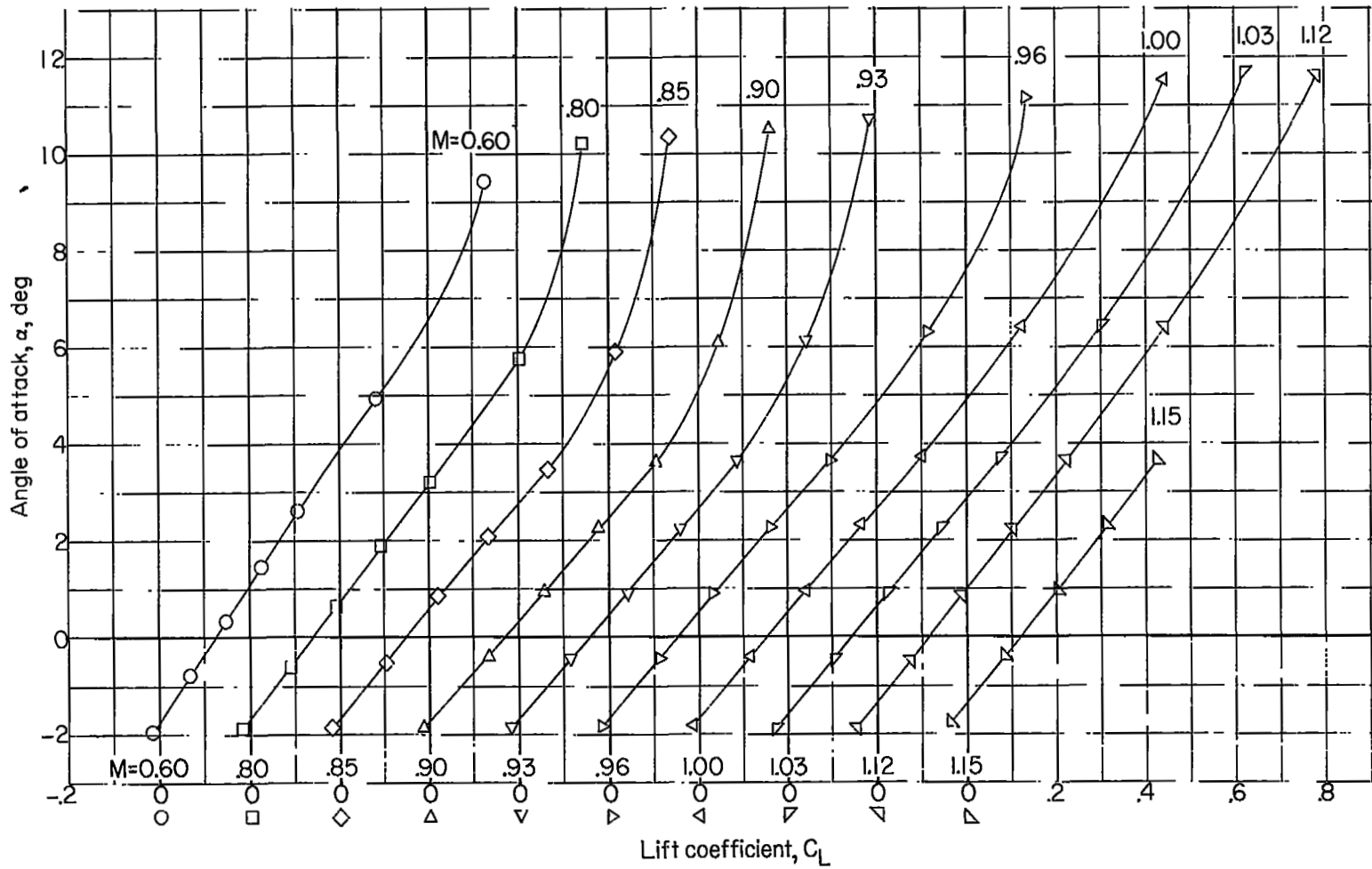
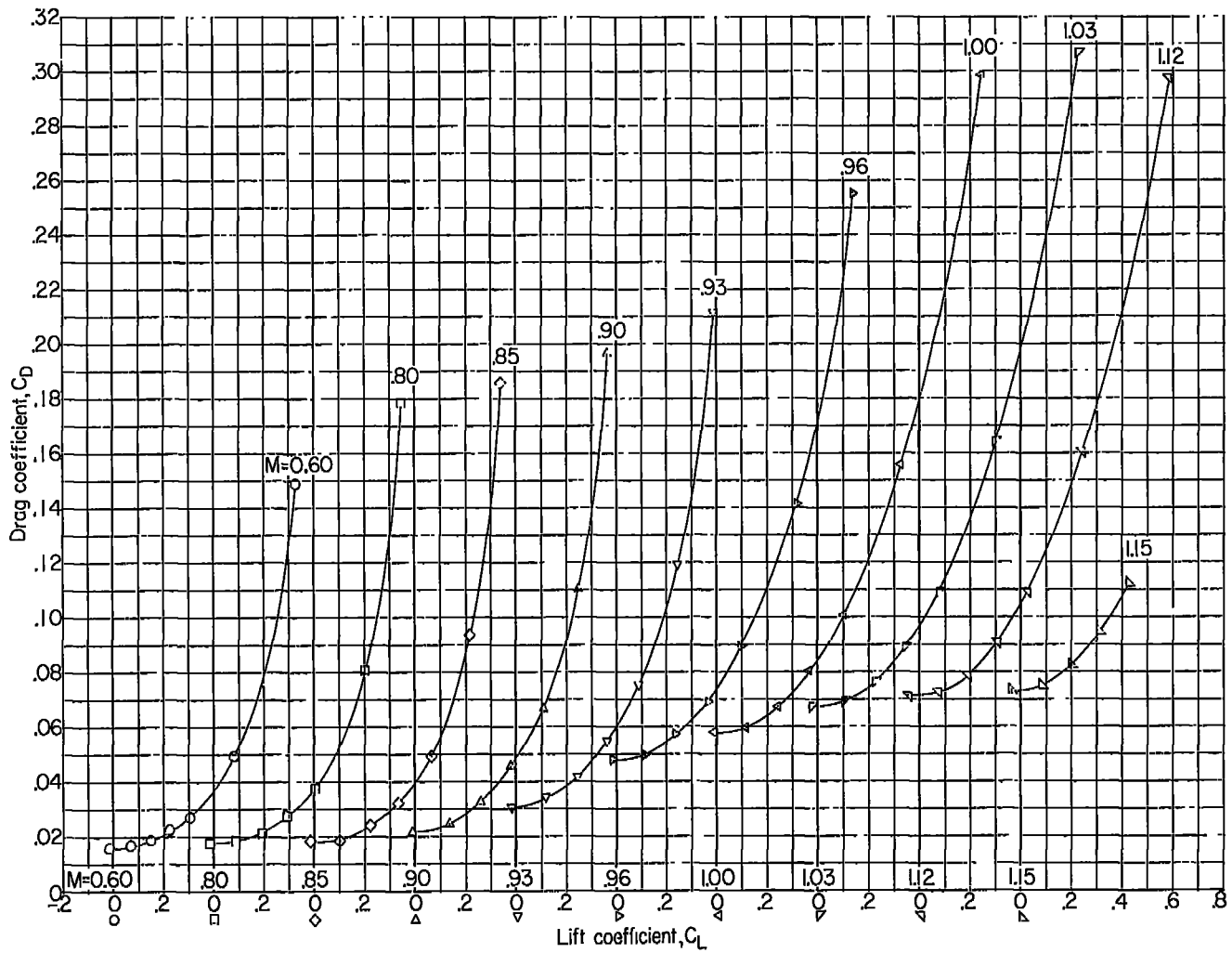


Figure 6.- Variation with Mach number of average test Reynolds number based on $\bar{c} = 5.46$ inches.



(a) α against C_L .

Figure 7.- Force and moment characteristics for the basic configuration without stores.



(b) C_D against C_L .

Figure 7.- Continued.

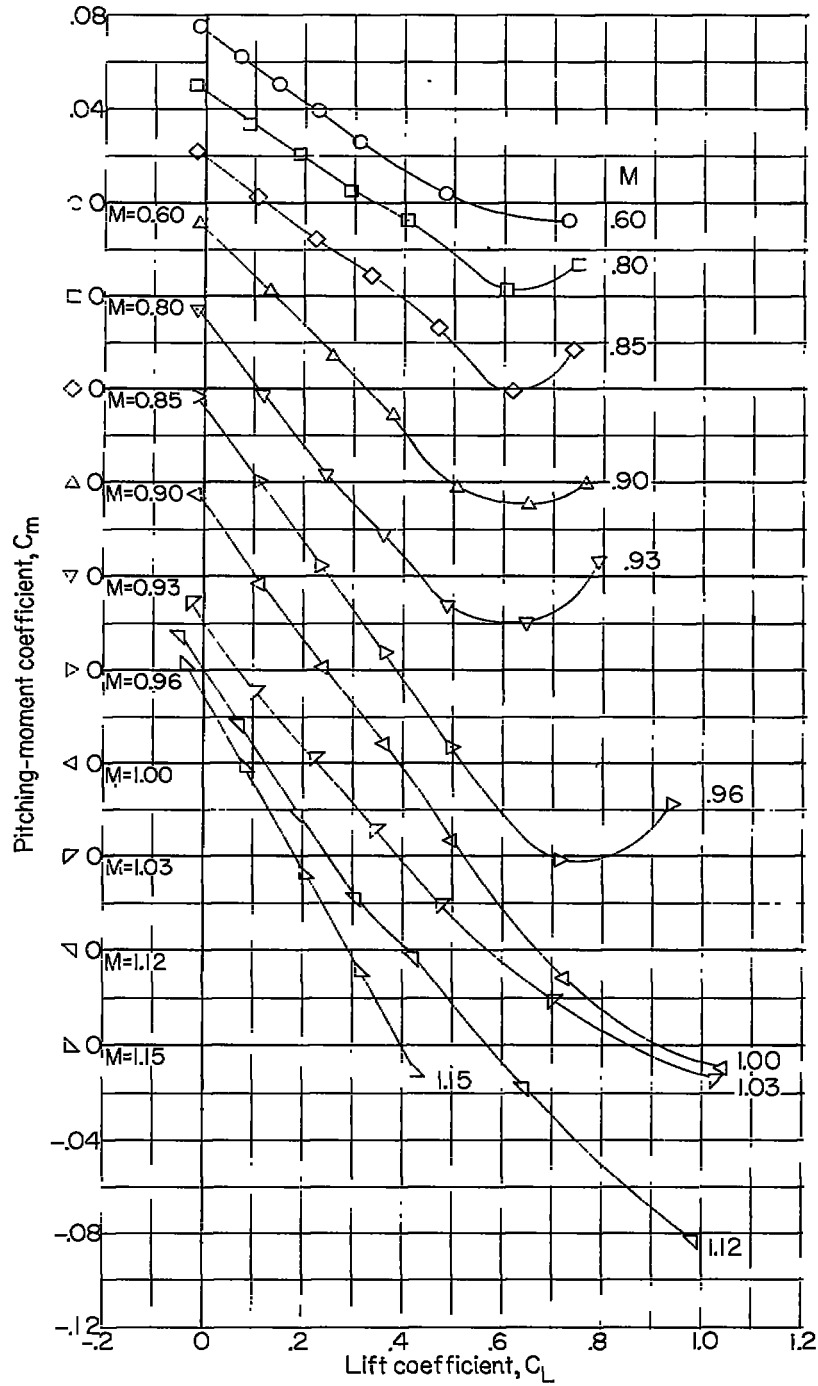
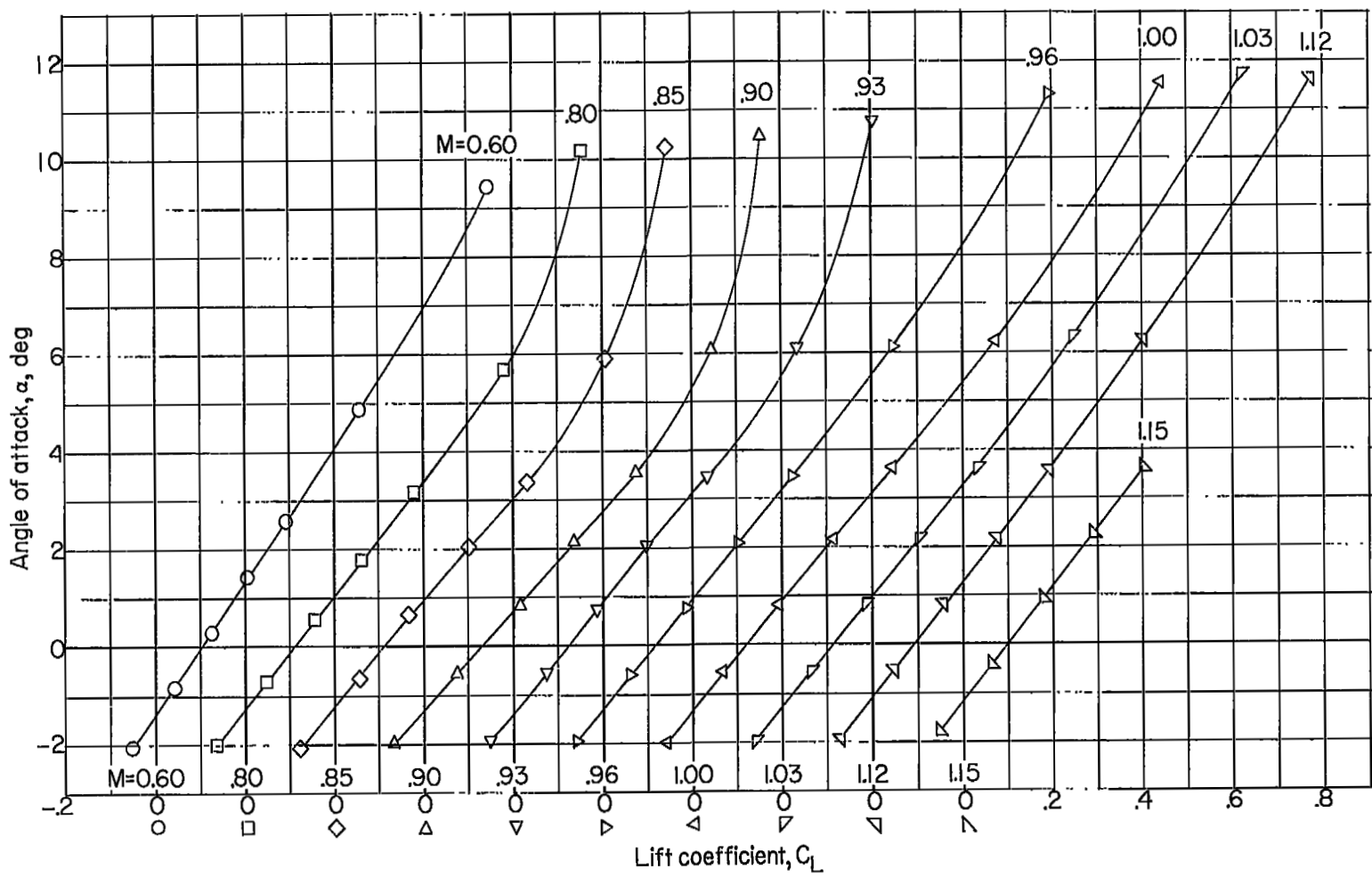
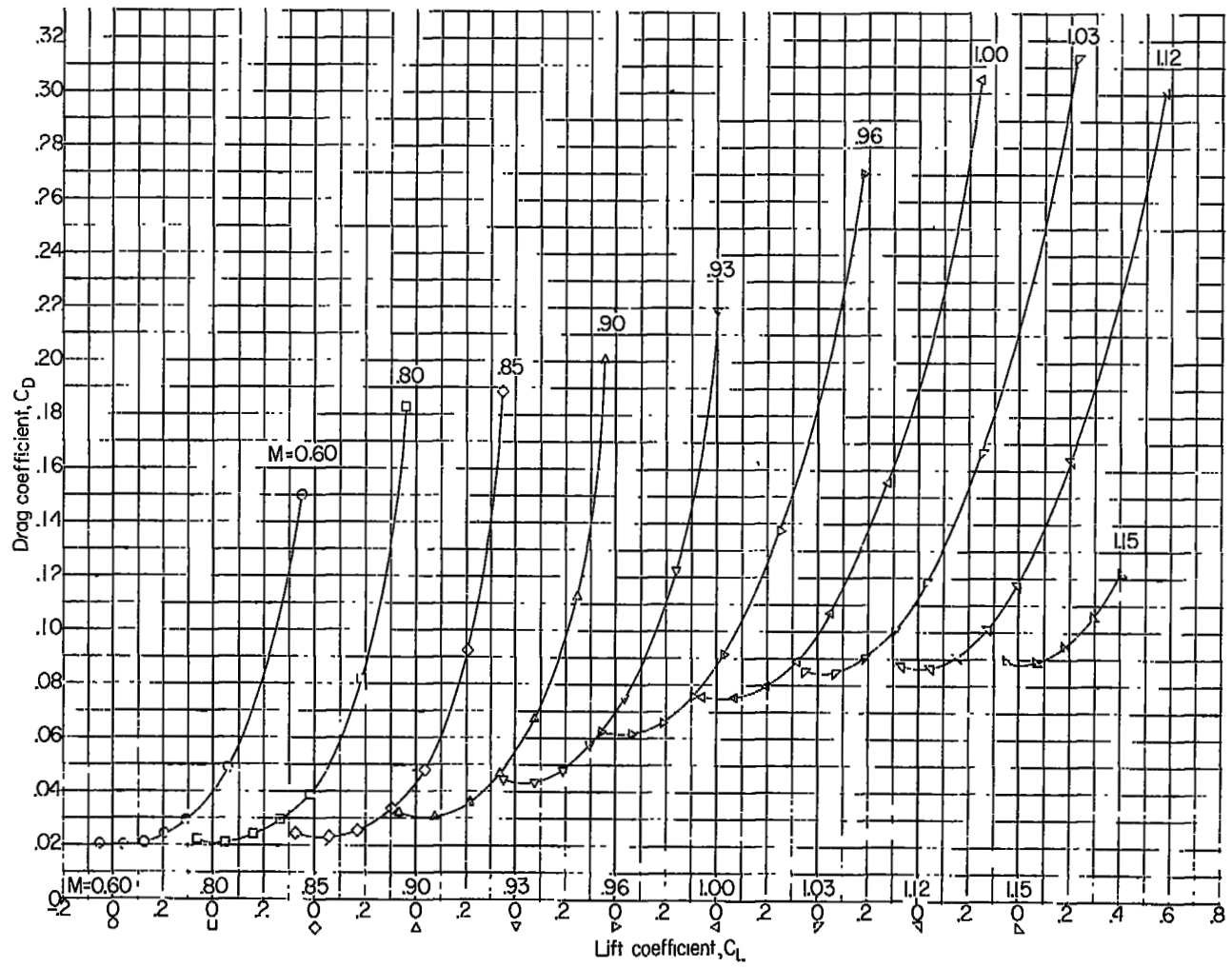
(c) C_m against C_L .

Figure 7.- Concluded.



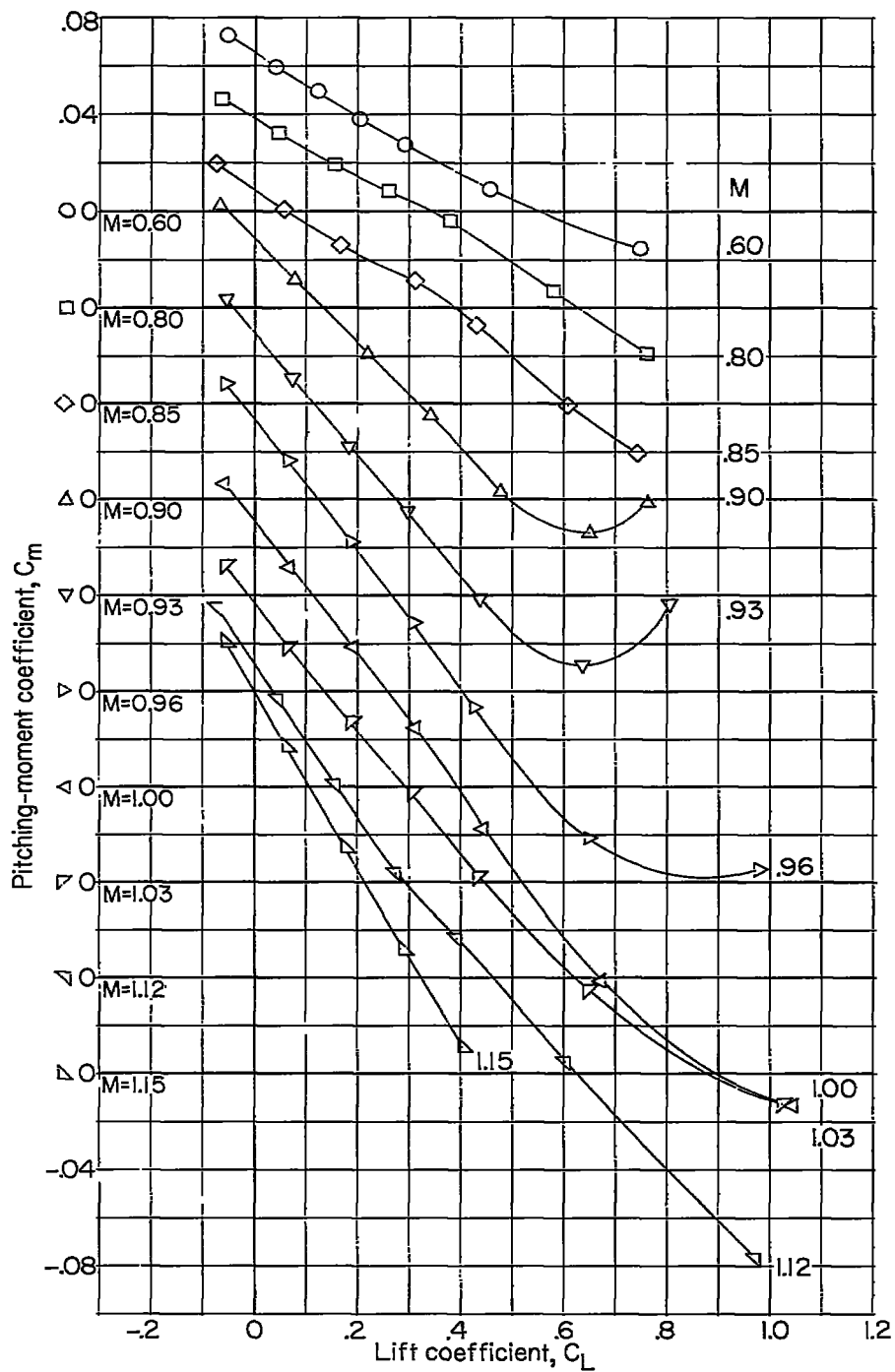
(a) α against C_L .

Figure 8.- Force and moment characteristics for the basic configuration tested with stores at the outboard (0.61-semispan) position.



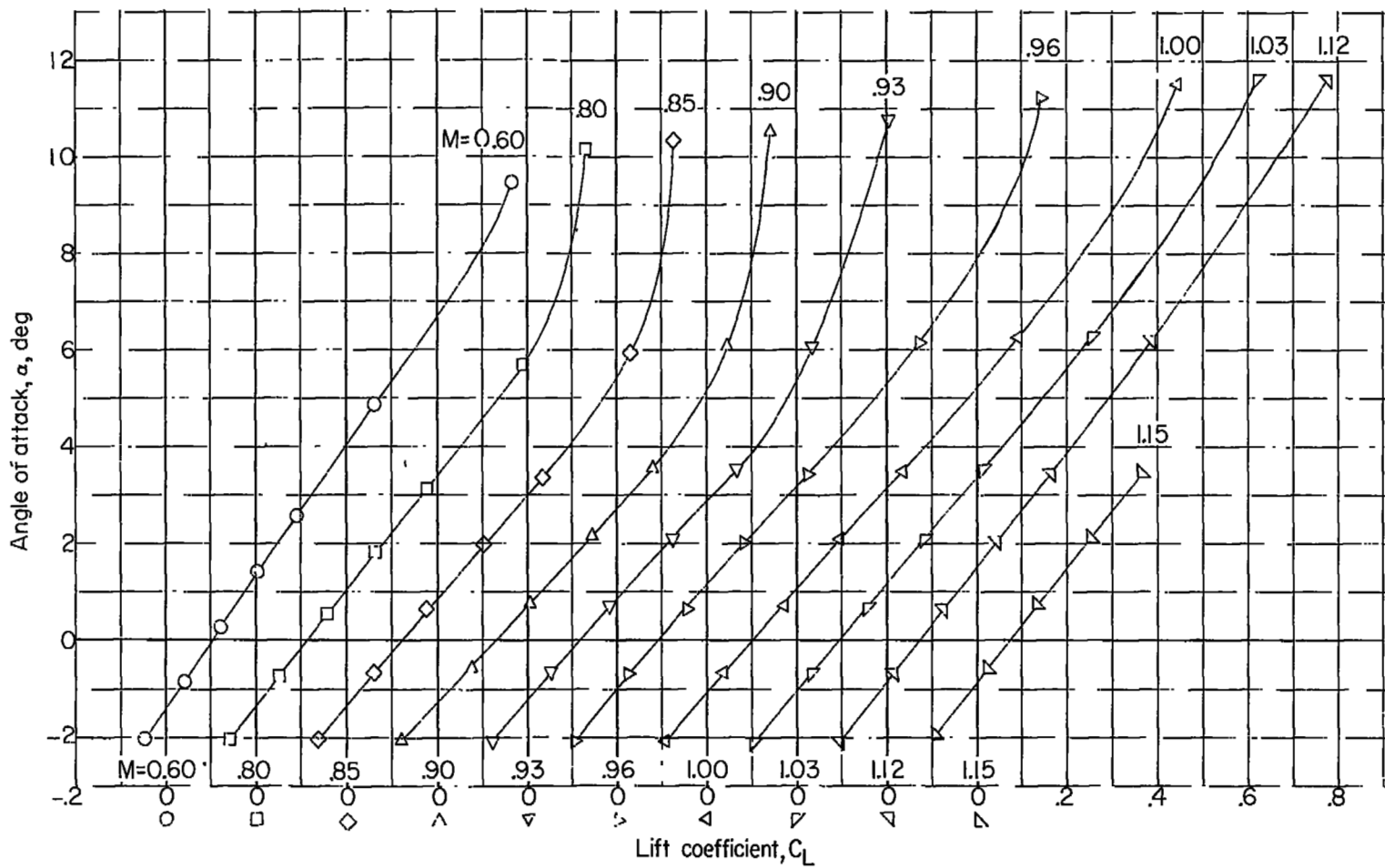
(b) C_D against C_L .

Figure 8.- Continued.



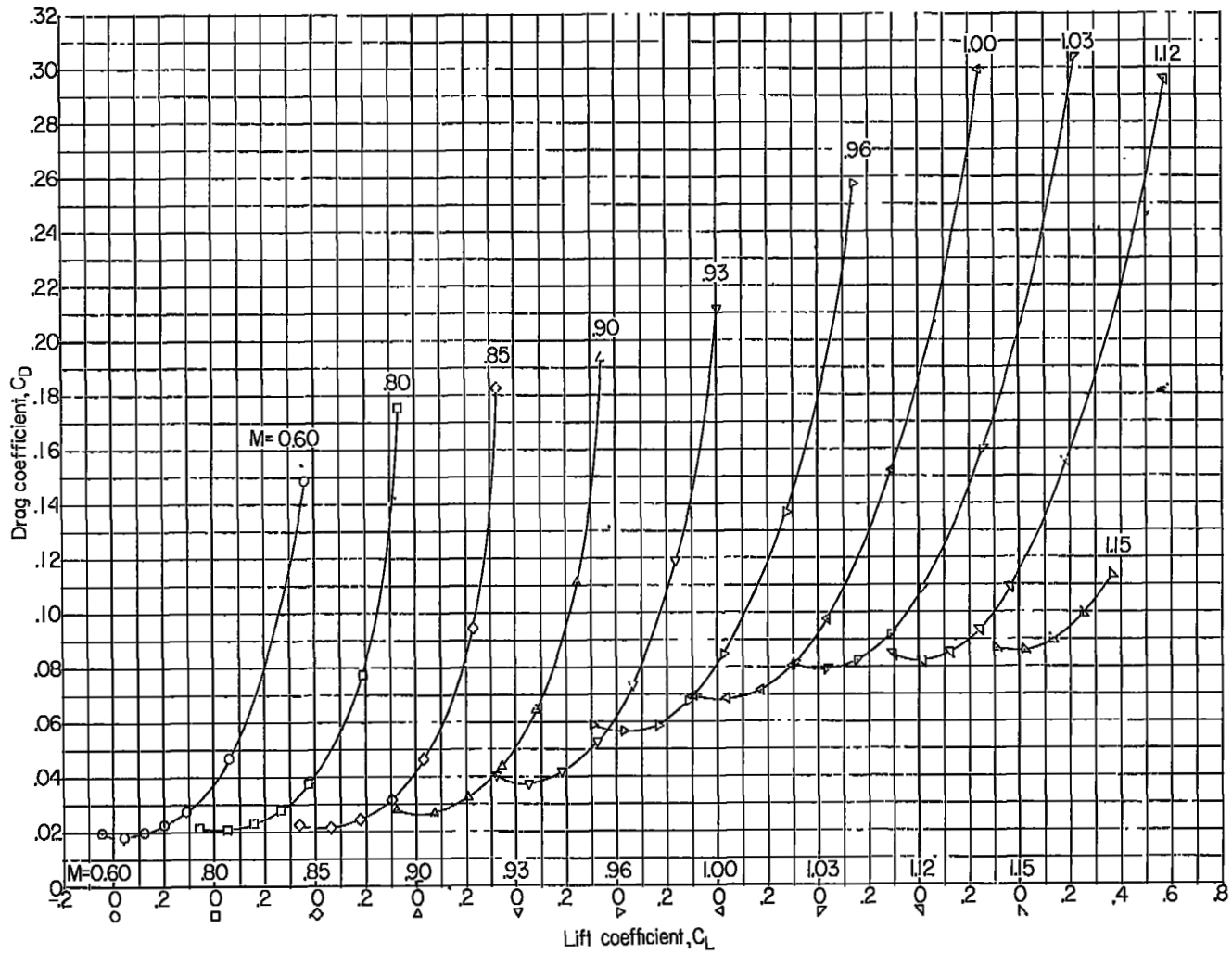
(c) C_m against C_L .

Figure 8.- Concluded.



(a) α against C_L .

Figure 9.- Force and moment characteristics for the basic configuration tested with stores at the inboard (0.44-semispan) position.



(b) C_D against C_L .

Figure 9.- Continued.

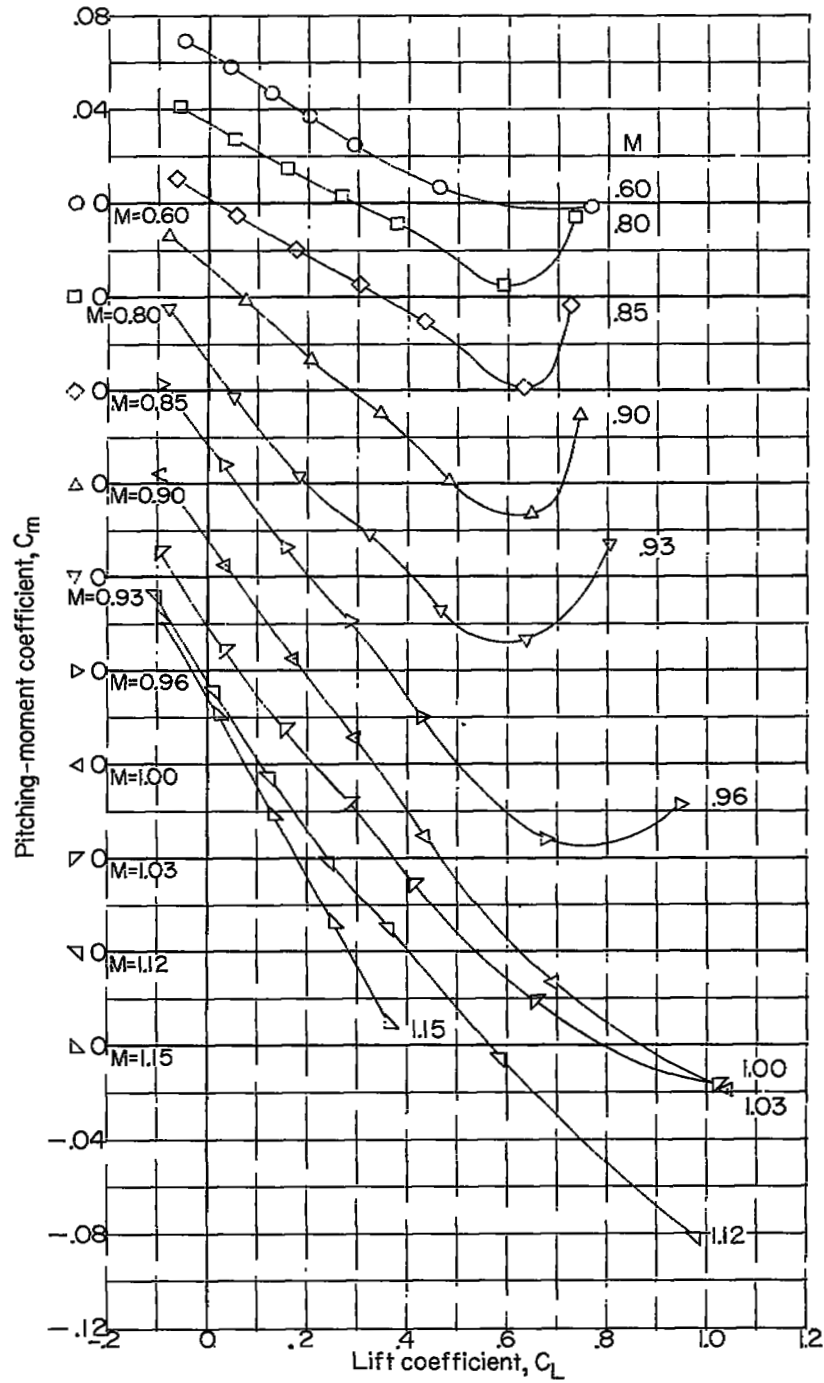
(c) C_m against C_L .

Figure 9.- Concluded.

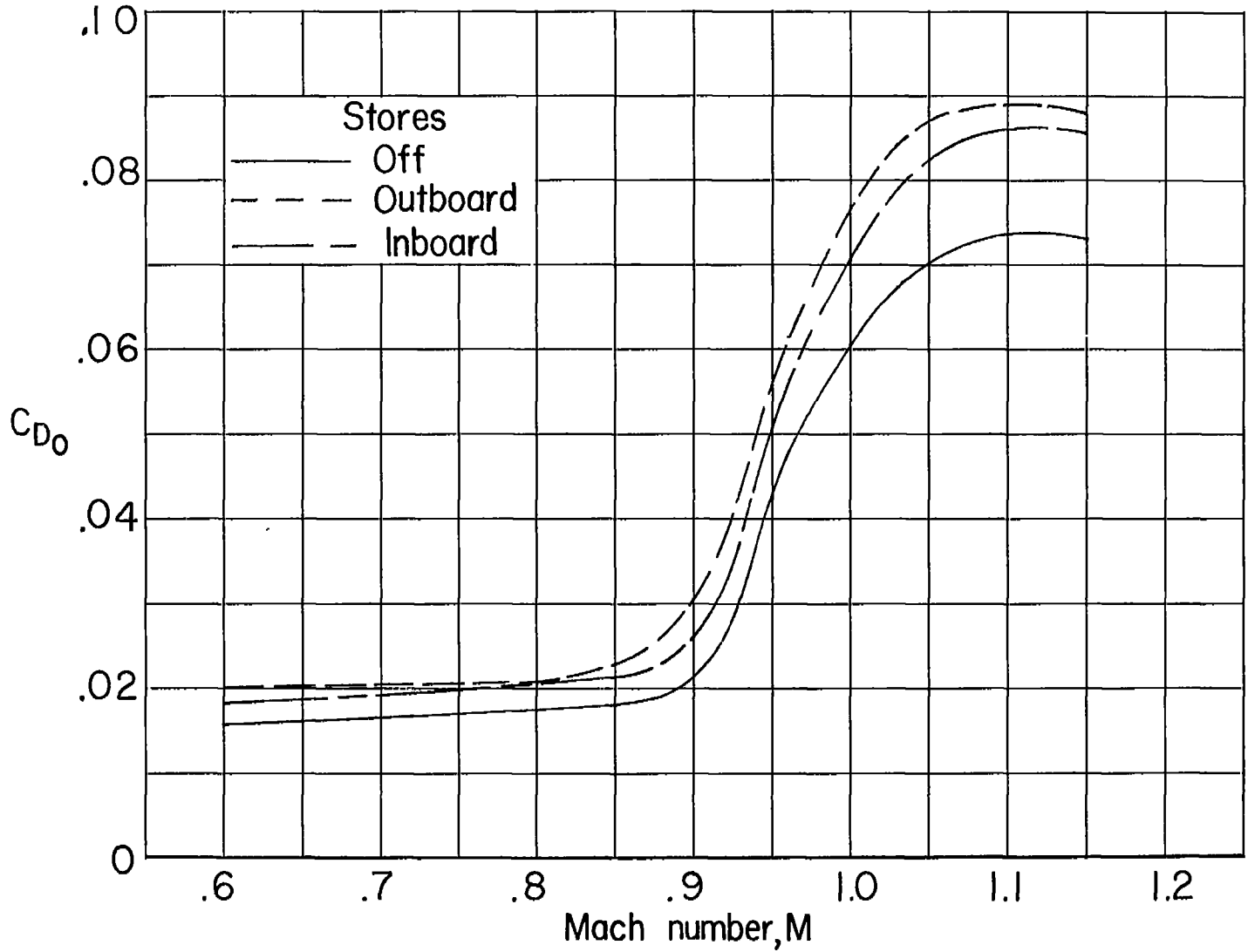


Figure 10.- Zero-lift drag coefficients for the model with and without stores.

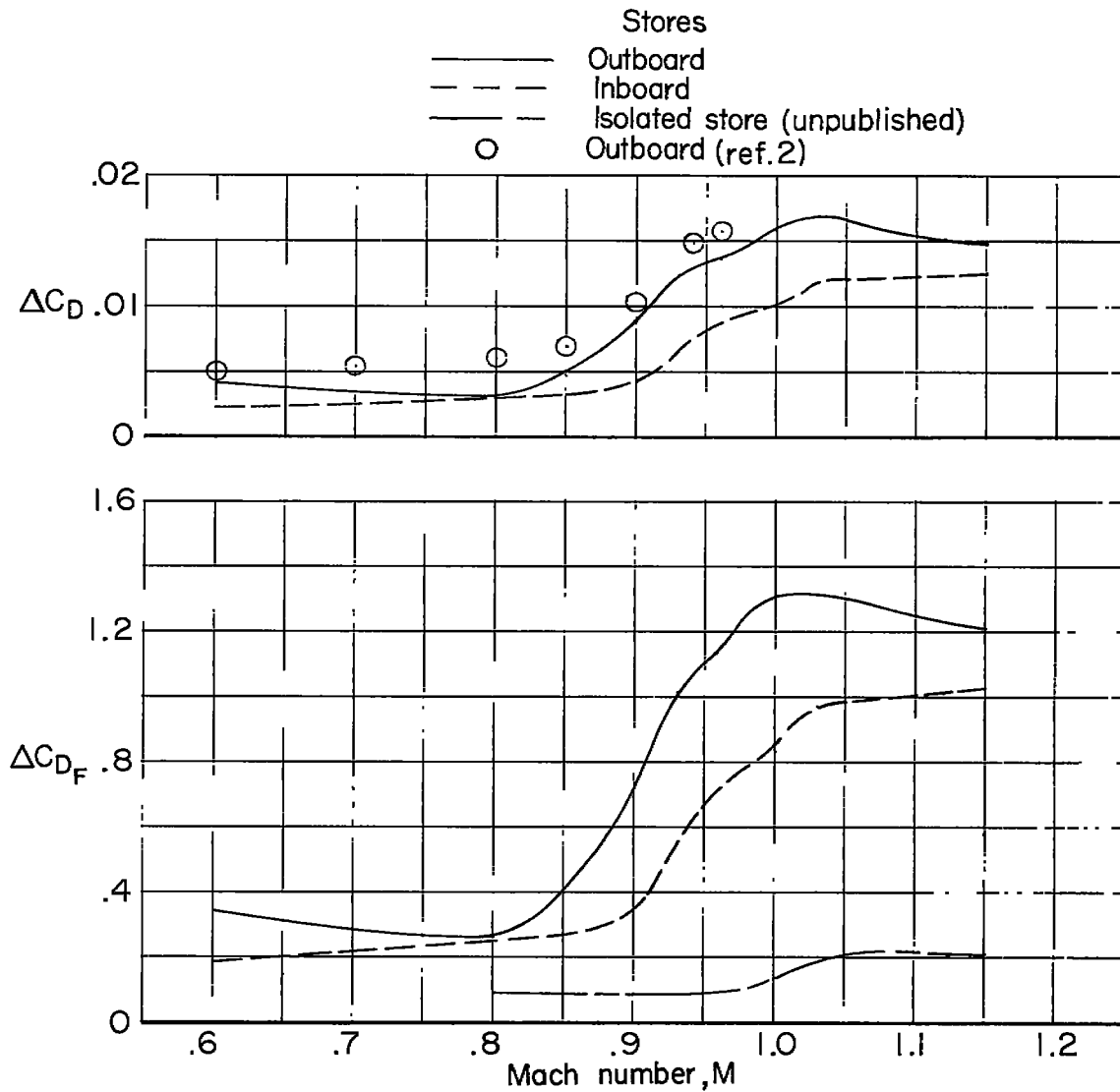


Figure 11.- Variation with Mach number of incremental drag coefficients due to adding stores. $C_L = 0$.

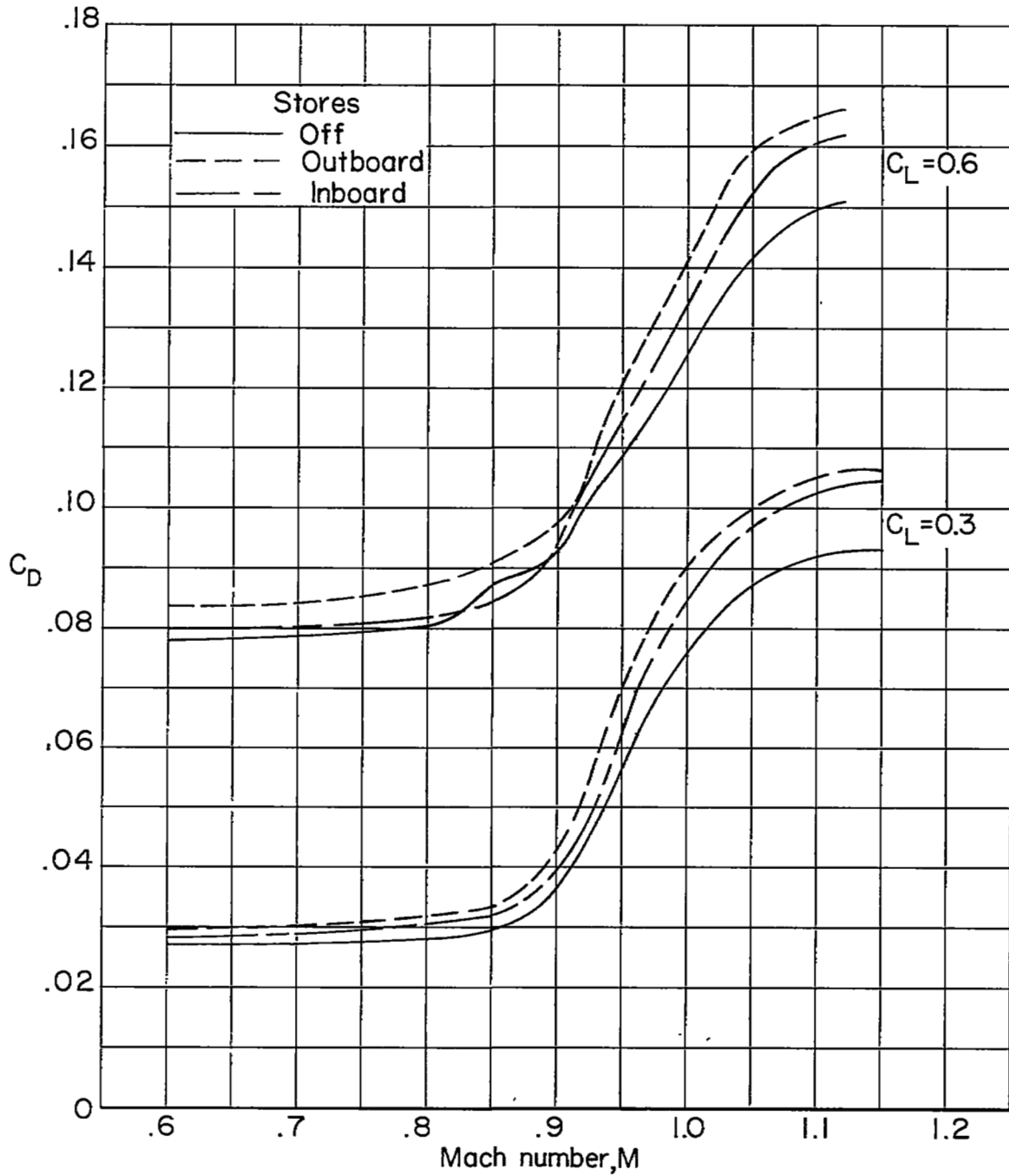


Figure 12.- Drag coefficients at constant lift coefficient for the model with and without stores.

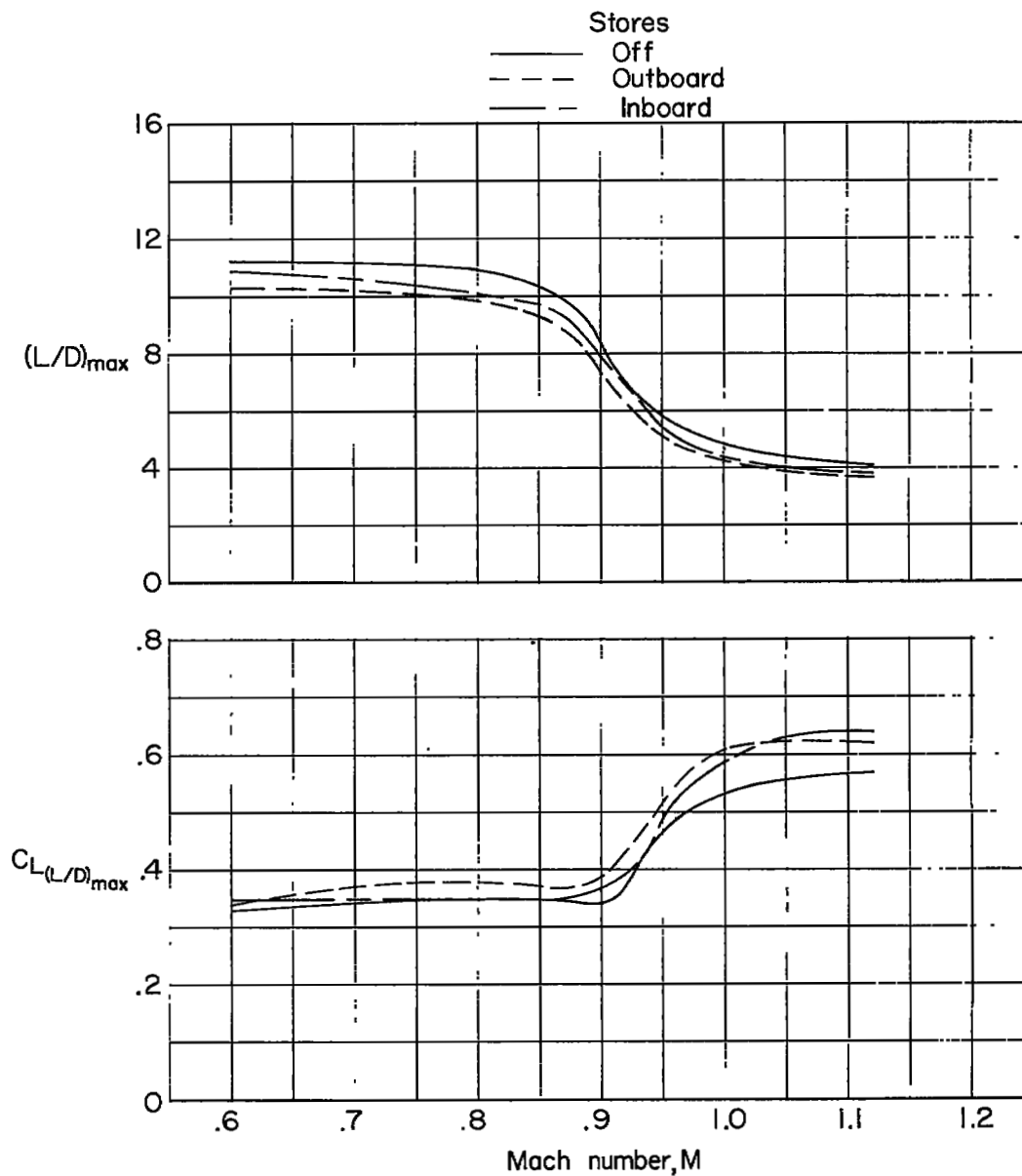


Figure 13.- Maximum lift-drag ratios and lift coefficients for maximum lift-drag ratio.

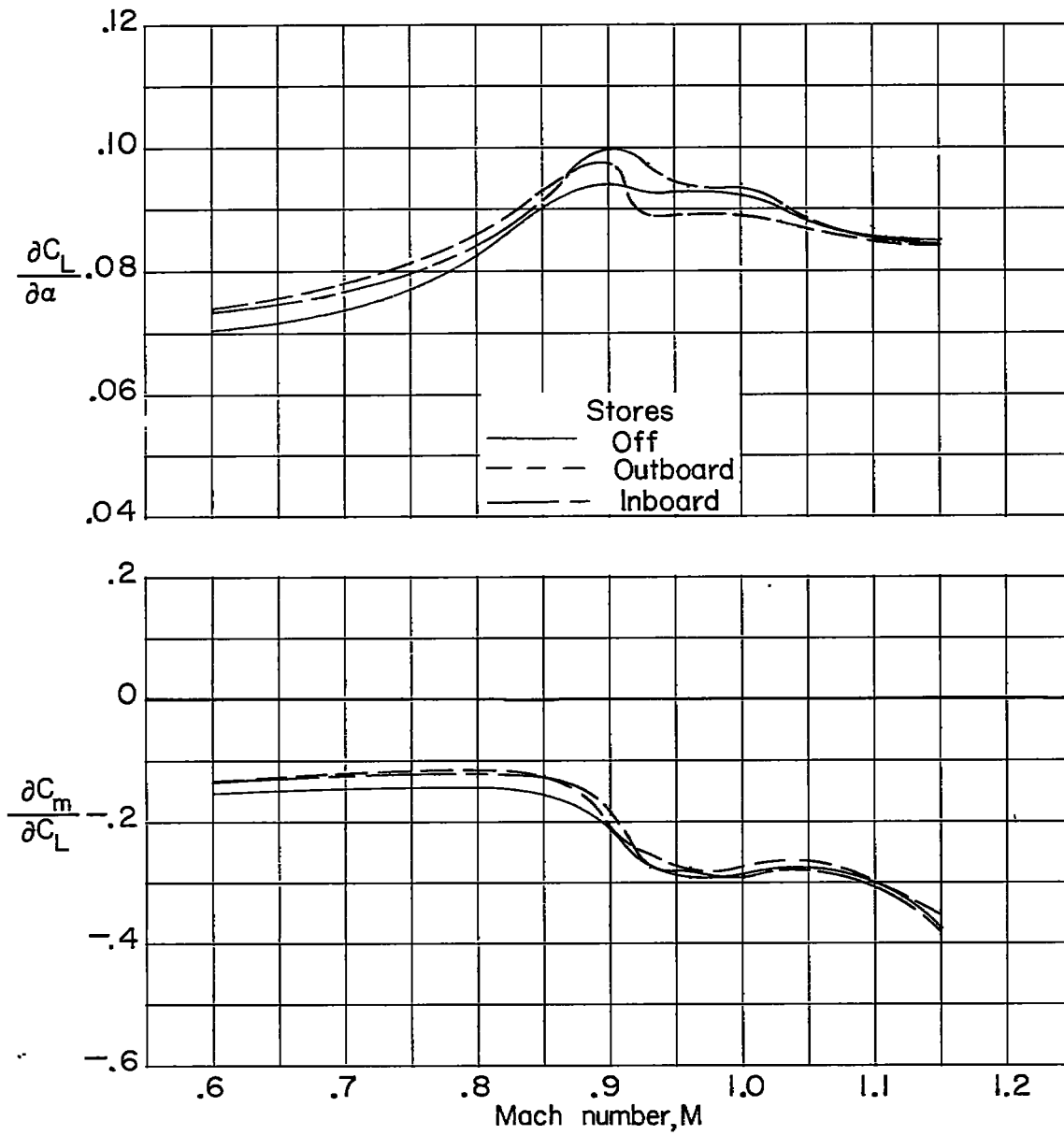


Figure 14.- Average lift-curve and moment-curve slopes for the model with and without stores.